IMPACT OF MODEL UNCERTAINTIES TO THE RECONSTRUCTION OF SURFACE PROFILES IN SCATTEROMETRY

Hermann Gross[1], Andreas Rathsfeld [2], Frank Scholze[1], *Markus Bär* [1]

[1] Physikalisch-Technische Bundesanstalt, Germany, Hermann.gross@ptb.de
[2] Weierstrass Institute for Applied Analysis and Stochastics, Germany, rathsfeld@wias-berlin.de

Abstract − Scatterometry is a non-imaging indirect optical method in wafer metrology to characterize periodic surface structures with dimensions in the micro- and nano-meter range. It is also important to lithography masks designed for extreme ultraviolet lithography (EUVL), where light with wavelengths in the range of 13 nm is applied. The solution of the inverse problem, i.e. the determination of periodic surface structures with respect to their critical dimensions (CD) and other profile properties from light diffraction patterns, is incomplete without knowledge of the uncertainties associated with the reconstructed parameters. With decreasing feature sizes of lithography masks, increasing demands on metrology techniques and their uncertainties arise. The numerical simulation of the diffraction process for periodic 2D structures can be realized by the finite element solution of the two-dimensional Helmholtz equation. The inverse problem can be formulated as a non-linear operator equation. The operator maps the sought mask parameters to the efficiencies of diffracted plane wave modes. The operator equation can be solved by optimization, i.e., minimizing the deviation of the calculated efficiency or phase shift values from the measured ones. Clearly, the uncertainties of the reconstructed profile parameters essentially depend on the uncertainties of the input data and can be estimated by various methods. A Monte Carlo procedure and an approximate covariance method is applied to evaluate the reconstruction algorithm. Particularly, we analyze the impact of uncertainties in the model parameters by the Monte Carlo method. Reconstruction results and their uncertainties are presented for the measurements of typical EUV masks. They are composed of 140 nm wide TaN absorber lines of about 80 nm height, a period of 420 nm, and with an underlying MoSi-multilayer stack of 49 periods.

Keywords: Scatterometry, inverse scattering, lithography masks

1. INTRODUCTION

In the semiconductor industry both the feature sizes and the admissible limits of measurement uncertainty decrease continuously. The evaluation of structure dimensions on photo-masks and wafers in lithography is an important application of scatterometry [1,2,3]. Besides conventional metrology techniques like atomic force, electron and optical microscopy, scatterometry is an important tool for the characterization of such structures [4,5].

Scatterometry is known as a collective term for several metrology methods, which may be generally described as measurement techniques for a quantitative evaluation of surface properties by angle-resolved characterization and analysis of light scattered from a surface under test. Since no imaging optics is used, the surface and shape have to be reconstructed from intensity and/or polarization data detected in the far field by solving an inverse problem. Several measurement modes can be classified as scatterometric techniques, e.g. the standard scatterometer, the spectroscopic reflectometer, the spectroscopic ellipsometer, and the ellipsometric scatterometer. For the measurements in the EUV range (0.7 nm to 35 nm wavelength) we use the standard scatterometry approach, i.e. non-specular diffracted light is measured for different wavelengths of the incoming radiation. The measurements are carried out using the EUV reflectometer shown in Fig. 1.
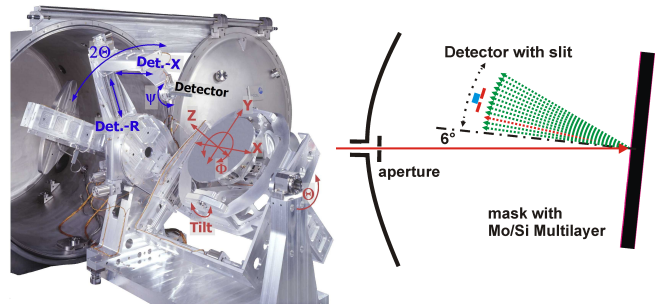

Fig. 1: Spectroscopic reflectometer [6] operating in the EUV range (0.7 nm to 35nm) and scheme of measurement set-up.

2. MODEL OF SCATTEROMETRY AND INVERSE PROBLEM

2.1. Profile model

In order to ensure a reasonable reconstruction accuracy, scatterometry requires a-priori information. Typically, the surface structure is sought in a certain class of profile structures described by a finite number of parameters, and these parameters are confined to certain intervals.

Fig. 2 shows such a class and its geometrical profile model for the cross-section over one period of a typical line-space structure for EUV lithography where the extreme

ultraviolet wavelength range is applied. The cross section of the line is a symmetric polygonal domain composed of three trapezoidal layers of different materials (TaO, TaN, and SiO_2). These trapezoids are defined by the Y- and by the X-coordinates of the corner points. Beneath the line-space structure there are two capping layers of SiO_2 and of Si followed by a MoSi-multilayer stack (MLS). The last consists of a periodically repeated group of a Mo layer, a Si layer, and two intermediate layers. Note that the MLS is added to enable the reflection of EUV waves.
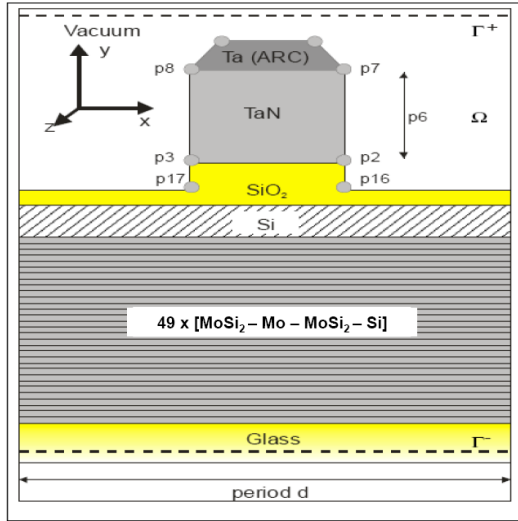

Fig. 2: Scheme of an EUV line-space structure composed of three trapezoidal absorber layers of different materials; the sought profile parameters are indicated.

Important geometric profile parameters are, e.g., the height p6 of the TaN absorber layer (55 - 60 nm) and the X-coordinates relative to the period p2 and p7 of the right corners of the TaN layer. In the following evaluations we assume a symmetric profile, i.e., the x-coordinates relative to the period of the corresponding left corner points p3 resp. p8 depend on those of the right corner points by p3 = 1-p2 and p8 = 1-p7. Furthermore we assume a fixed side wall angle (SWA) for the TaO layer of 82.6 degrees representing a certain edge rounding, i.e., the cross-section area of this trapezoidal layer is equal to a corresponding TaO layer having curved upper edges with a radius of about 6 nm. Additionally, the SWA of the SiO_2 layer should be always equal to the SWA of the TaN layer above. For all other model parameters, including the optical indices of the materials and the widths in the capping or the multilayer system, we suppose known values, i.e., they are fixed and will not be sought by our reconstruction method.

2.2. Helmholtz equation

The evaluation of geometrical profile parameters from measurement data depends crucially on a rigorous modelling by Maxwell's equations and on accurate numerical algorithms. Note that Maxwell's equations in the time-harmonic case reduce to the two-dimensional Helmholtz equation (1) if geometry and material properties are invariant in one direction. Fig. 3 shows a scheme for the irradiation of a periodic surface structure. For the numerical solution, a lot of methods have been developed [7-10]. We use the finite element method (FEM) and truncate the infinite domain of computation to a finite one by coupling with boundary elements. To compute highly oscillatory fields, generalized finite element methods are available [11]. Coupling the FEM solution of this boundary value problem with the so-called Rayleigh expansion of $u(x, y)$ provides a general solution above and below the mask for the outgoing wave modes.

$$\Delta u(x, y) + k^2 u(x, y) = 0 \qquad (1)$$

Here the wave number $k = k(x, y) = \omega \sqrt{\mu_0 \varepsilon(x, y)}$ is constant in each area of the mask specimen filled by the same material, and ω is the circular frequency of the incident plane wave.
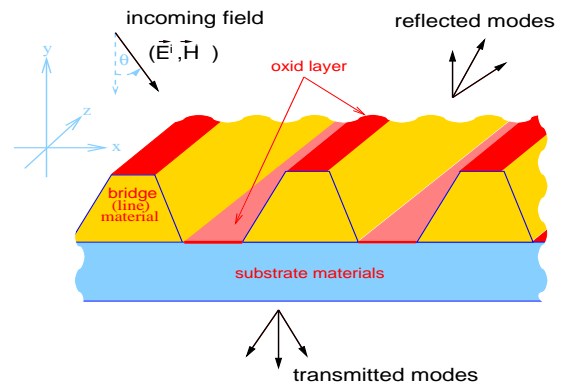

Fig. 3: Scheme for wave interaction with a periodic grating structure with homogenous material properties in z direction.

2.3. Profile reconstruction by optimization

Apart from the forward computations of the Helmholtz equation, the solution of the inverse problem, i.e. the reconstruction of the grating profiles and interfaces from measured diffraction data, is the essential task in scatterometry. This problem is similar to the optimal design of diffractive optics. The inverse problem can be formulated as a non-linear operator equation. The operator maps the sought mask parameters to the efficiencies of diffracted plane wave modes. The operator equation can be solved by optimization, i.e., minimizing the deviation of the calculated efficiency or phase shift values (e_n) from the measured ones (E_n):

$$f(p_j) := \chi^2(p_j) = \sum_n \frac{1}{u_n^2} \left[e_n(p_j) - E_n \right]^2 \qquad (2)$$

If the uncertainties of the measured values are available, then it is common for such least-square procedures to

choose weighting factors as the squared reciprocal uncertainties (u_n^{-2}).

The values of the sought profile parameters $\{p_j\}$ are varied until the minimum of the functional (2) has been found. Our approach here employs a Gauß-Newton type iteration proposed e.g. by Al-Assaad and Byrne [12] and is based on FEM computation for the efficiencies of the line-space structure and for their derivatives with respect to the profile parameters [13]. It is well known that the solution of the inverse problem might fail if it is based on insufficient or improper input data. Studies with simulated data for a typical grating representing a photolithographic mask [5,14] show a strong dependence of the reconstruction result on the subset of efficiencies chosen from the set of all available efficiencies.

3. RESULTS: MEASUREMENT UNCERTAINTIES FROM MULTILAYER PERTURBATIONS

3.1. Influence of detector uncertainties

Clearly, the measured efficiency values E_n entering the numerical algorithm have uncertainties and will influence the accuracy of the reconstructed parameter values. To analyze this, a simple noise model for the detected efficiencies is considered: Suppose that systematic effects can be neglected and that the values of uncertainty contribution to E_n are normally distributed (Gaussian) with zero mean and standard deviation given in equation (3).

$$u_n = \sqrt{\left(a \cdot E_n\right)^2 + \left(b_g\right)^2} \qquad (3)$$

Then, one identifies the uncertainties of the input data with u_n. The first term $a \cdot E_n$ represents a linearly dependent noise with a constant factor a (e.g. $a = 0.01$). The second term accounts for a background noise independent of the measured efficiencies or phase shifts (typical value of b_g is 10^{-5}, i.e., $b_g = 0.001$ %).

In [14] we compare the results obtained from a Monte Carlo procedure to the estimations gained from the approximate covariance matrix of the profile parameters close to the optimal solution. The numerical examples in this study use EUV line-space structures which are very similar to those schematically shown in Fig. 2. For all parameters investigated and reconstructed with simulated measurement data and even for suitable data sets with a moderately reduced number of measurement values, the relative uncertainties have been found to be smaller than 2 %. Of course, these results are valid under the assumption, that the uncertainties resulting from the inaccuracies in the geometric modelling of the line-space structure are neglected respectively are much smaller than the uncertainties of the measured efficiencies or phase shifts, ranging from 1 to 3 % in the numerical examples.

3.2. Influence of multilayer perturbations

In further investigations the impact of effects like non-periodic details of real mask structures, e.g., perturbations in the periodicity of the multilayer system beneath the line-space structure, on the uncertainties of the reconstructed parameters have been examined.

Obviously, the reconstruction results do not only depend on the uncertainties of the measured efficiencies, but on the so far fixed model parameters too. The capping and multilayer system, determined independently from the parameters of the line-space structure by evaluation of bright-field measurements, will be shown to be crucial for the final reconstruction of the parameters of the line-space structure.

In order to get assessments about the influence of the MLS and capping parameters on the reconstruction results, we applied the Monte Carlo method. That means, we generate stochastic capping layer/MLS models such that the layer widths are normally distributed independent variables. Based on these models, we ran our reconstruction algorithm for the geometric parameters of the line-space structure. Finally, we got the distributions of the sought profile parameters in dependence on the capping layer/MLS models. The nominal thickness values for the capping layer/MLS were determined independently by evaluation of bright field reflectance measurements [15].

We have examined the noise levels given in the first column of Table 1. Different perturbations for the widths of the capping layers resp. the widths in the MLS allow to separate the impacts of these components. For each of the given fluctuations, the standard deviations of the relative x-coordinates of the corner points p2 and p7 as well as that of the height p6 were calculated. Furthermore the standard deviations of the SWA and of the horizontal line widths in the middle of the height of the absorber line, indicated as CDm, were calculated. These parameters are easy to calculate from the reconstructed profile parameters p2, p7, and p6. Additionally, the impact of an offset of ±5% for the capping layers relative to their nominal values has been studied and the results are given in the last two rows of Table 1.

For all results presented in Table 1, we have used the medium-sized measurement data set indicated as N2m-25 and composed of 25 efficiencies including the diffraction orders from -4 to +4 resp. -4 to +2 at wave lengths of 13.4nm, 13.7nm, and 13.9nm. The mask field inspected by the EUV light had a nominal line width of 140 nm and a period of 420 nm corresponding to a line to space ratio of 1:2. The reconstructed profile parameters for the reference values are given in Table 2, and the standard deviations in Table 1 are those of the fluctuation around these reference values.

It is striking to note that for all examined perturbations the standard deviation of the height p6 of the absorber line is significantly smaller than the deviations for the corner points. This was to be expected due to the higher sensitivity of the height p6 with respect to the reflected wave modes. We have observed a similar trend for the standard deviations in dependence on different noise levels of the measured efficiencies (cf. [14]).

As a consequence of the larger deviations in the horizontal X-coordinates, the standard deviations for the SWA are relatively large and always greater than 1.5^0. Furthermore it can be observed that, for perturbed MLS widths smaller than 0.5%, the horizontal width at the middle of the height (CDm) has relatively small deviations indicating a stable value. In other words, the reconstruction of CDm is just as stable as that of p6.

An offset of 5% for the widths of capping layers (cf. last two rows of Table 1) does not affect significantly the standard deviations of the reconstructed parameters. However, a systematic shift of the reconstructed SWA appears. In fact, the SWA increases significantly if the SiO_2 and Si capping layers are presumed to be thinner than the corresponding reference values of 1.234 nm and 12.869 nm, measured by reflectometry in open MLS test structures without absorber lines. The mean side-wall angle increases to 87.8^0 compared with 85.0^0 for the reference thickness values. The SWA angle measured by atomic force microscopy is between 86.9° and 87.6°.

Table 1. Monte Carlo results for perturbed capping layer/MLS models: Applied to reconstruction of a measured EUV mask (period 420 nm, line to space ratio 1:2).

Perturbation Cap./ MLS	σ_2 /nm	σ_6 /nm	σ_7 /nm	σ_{SWA} /^{o}	σ_{CDm} /nm
1% / 0.1%	0.86	0.10	0.67	1.52	0.11
1% / 0.5%	1.35	0.29	1.24	2.30	1.19
1% / 1.0%	2.15	0.47	1.79	2.75	2.81
2% / 0.1%	1.21	0.21	0.85	2.06	0.25
2%-5% / 0.1%	1.37	0.24	0.81	2.16	0.41
2%+5% / 0.1%	0.95	0.36	0.77	1.72	0.17

Table 2. Reconstructed geometrical parameter values of a medium-sized data set (N2m-25): Period 420 nm, line to space ratio 1:2, cap. layer widths [1.234 nm, 12.869 nm], MLS widths 49x[0.147 nm, 2.141 nm, 1.972 nm, 2.838 nm].

p_2-p_3 /nm	p_6 /nm	p_7-p_8 /nm	SWA /^{o}	CDm /nm
157.7	57.19	143.1	85.0	150.92

4. CONCLUSIONS

Clearly the uncertainties of the reconstructed parameters depend on the uncertainties of the input data for the reconstruction algorithm. We have analyzed the influence of certain presumed and fixed model parameters, namely, the thicknesses of the two capping layers and the four widths in the periodically repeated groups of the multilayer system. In order to restrict the amount of work, we have confined our test to a single medium-sized measurement data set. It turned out, that the impact of such model uncertainties is crucial. It leads to a rise in the uncertainties of up to 3% for all parameters investigated and is thus at least comparable to the detector-noise related uncertainties. Furthermore, it induces systematic shifts of the results as discussed here for the capping layer thickness and SWA. The CD for the

bottom and the top of the line-space structure show significantly increased variations. Even for the smallest presumed perturbation (capping layer thickness perturbed by 1% and MLS layers by 0.1%), the standard deviation of the side-wall angle is greater than 1.5^0. On the other hand, we have observed that the height of the line-space structure and its mean CD are relatively stable with respect to the studied model based uncertainties. Furthermore, our examinations have revealed a strong correlation between the thicknesses of the capping layers, e.g. the SiO_2 layer, and the side-wall angle.

REFERENCES

[1] B.K. Minhas. et al., "Ellipsometric scatterometry for metrology of sub-0.1um-linewidth structures", Appl. Optics, 37, No. 22, pp. 5112-5115, 1998.

[2] C.J. Raymond et al., "Multiparameter grating metrology using optical scatterometry", J.Vac.Sci.Technol., 15 (2), pp. 361-368, 1997.

[3] C.J. Raymond et al., "Metrology of sub-wavelength photoresist gratings using optical scatterometry", J. Vac. Sci. Technol., 13 (4), pp. 361-368, 1995.

[4] M. Wurm et al., "Evaluation of scatterometry tools for critical dimension metrology", DGaO Proceedings, 106, 2005.

[5] H. Gross et al., "Mathematical modelling of indirect measurements in scatterometry", Measurement, 39, pp. 782-794, 2006.

[6] J. Tümmler, at al., "New PTB reflectometer for the characterization of large optics for the extreme ultraviolet spectral region", Proc. SPIE 4688, 338-347, 2002

[7] M-G. Moharam et al, "Stable implementation of the rigorous coupled-wave analysis for surface-relief gratings: enhanced transmittance matrix approach", JOSA A 12, pp. 1077-1086, 1995.

[8] L. Li, "New formulation of the Fourier modal method for crossed surface-relief gratings", JOSA A 14, pp. 2758-2767, 1997.

[9] J. Chandezon et al., "A new theoretical method for diffraction gratings and its applications", J. Opt. (Paris), 11, pp. 235-241, 1980.

[10] B.H. Kleemann, "Elektromagnetische Analyse von Oberflächengittern von IR bis XUV mittels einer parametrisierten Randintegralmethode: Theorie, Vergleich und Anwendungen", Dissertation, TU Ilmenau (2002),

[11] J. Elschner et al., internet DIPOG Homepage, http://www.wias-berlin.de/software/DIPOG.

[12] R.M. Alassaad and D.M. Byrne, "Error Analysis in Inverse Scatterometry I: Modeling", JOSA A 24, pp.326-338, 2007.

[13] J. Elschner and G. Schmidt, ``Conical diffraction by periodic structures: Variation of interfaces and gradient formulas", Math.Nachr., 252, pp. 24-42, 2003.

[14] H. Gross et al., "Computational methods estimating uncertainties for profile reconstruction in scatterometry", Proc. of SPIE, 6995, pp. 0T1-0T9, 2008.

[15] J. Perlich et al., "Characterization of extreme ultraviolet masks by extreme ultraviolet scatterometry", J. Vac. Sci. Technol., pp. 3059-3062, 2004.